Simple metamaterial structure enabling triple-band perfect absorber

2015 J. Phys. D: Appl. Phys. 48 375103

(http://iopscience.iop.org/0022-3727/48/37/375103)

IOP Publishing Journal of Physics D: Applied Physics
J. Phys. D: Appl. Phys. **48** (2015) 375103 (6pp) doi:10.1088/0022-3727/48/37/375103

Simple metamaterial structure enabling triple-band perfect absorber

Nguyen Van Dung[1], Bui Son Tung[1], Bui Xuan Khuyen[1], Young Joon Yoo[1], Young Ju Kim[1], Joo Yull Rhee[2], Vu Dinh Lam[3] and YoungPak Lee[1]

[1] Department of Physics, Quantum Photonic Science Research Center and RINS, Hanyang University, Seoul 133-791, Korea
[2] Sungkyunkwan University, 25-2 Sungkyunkwan-ro, Jongno-gu, Seoul, Korea
[3] Institute of Material Science, Vietnamese Academy of Science and Technology, Hanoi, Vietnam

E-mail: yplee@hanyang.ac.kr

Received 17 March 2015, revised 28 June 2015
Accepted for publication 21 July 2015
Published 21 August 2015

Abstract

Two resonators in metamaterial usually correspond only to two absorption peaks. In this report, by breaking the symmetry, we could create multi-fundamental resonances at GHz frequencies in both simulation and experiment. First, a dual-band metamaterial absorber (MA) was achieved for 4.6 and 10.6 GHz. Next, by modifying the relative position of inner square, the triple-band MA was obtained with enhanced absorption properties. In addition, dependence on the polarization of the incident electromagnetic (EM) wave was clarified. The mechanism is elucidated to be an alteration of the coupling strength, which is made by changing the geometrical configuration of the inner square and the outer ring. It is shown that our structural configuration can be applied to the fields where the interaction with a wide range of EM waves exists or is needed.

Keywords: metamaterial, perfect absorber, electromagnetically-induced transparency, symmetry breaking

(Some figures may appear in colour only in the online journal)

In view of improved performance and a variety of real applications, such as sensors [1, 2], camouflage [3] and wireless communication [4], materials with high absorption have been a domain which has attracted interest from scientists and engineers. Recently, in striking contrast to the conventional material, metamaterial absorbers (MAs) are rising as promising artificial materials which provide peculiar electromagnetic (EM) properties, not only for EM absorbers but for negative permittivity and/or permeability etc. The field of metamaterials (MMs) is growing rapidly owing to developing desired types of manufacturing materials, which work at radio, microwave and, later, optical frequencies [5–9]. Landy *et al* proposed a MM structure manipulating the effective parameters to be impedance-matched with the outside environment and for the proper loss enhancement [10]. In the past several years, MM absorbers have been suggested for GHz, THz and optical frequency regimes [11–14]. It is clear that MM absorber is due the EM resonances and that the number of absorption peaks depends on the number of resonant modes of the structure. Therefore, several structures providing dual band, triple band and multi-band, have been developed, based on the aforementioned mechanism [13, 15–17]. In 2014, Wang *et al* proposed a structure with two rings to create a triple band by breaking symmetry, but this double ring structure has shown polarization dependence and is without experiment verification [11].

In this report, we present the numerical design and the experimental demonstration of dual- and triple-band nearly-perfect MM absorbers using the simple sandwich structure. The unit cell of front patterns consists of inner and outer squares. At first, dual-band MM absorber was achieved at 4.6 and 10.6 GHz with absorption of 99.5% and 77.2%, respectively. Next, by changing the relative position of inner square, dual-band MM absorber was obtained with the absorption enhancement of the second peak. When the displacement of inner square, d, is big enough, the second peak is separated into two peaks. The influence of polarization and incident angle of EM wave is also examined, to show that our structure is polarization- and incidence-insensitive to the EM wave.

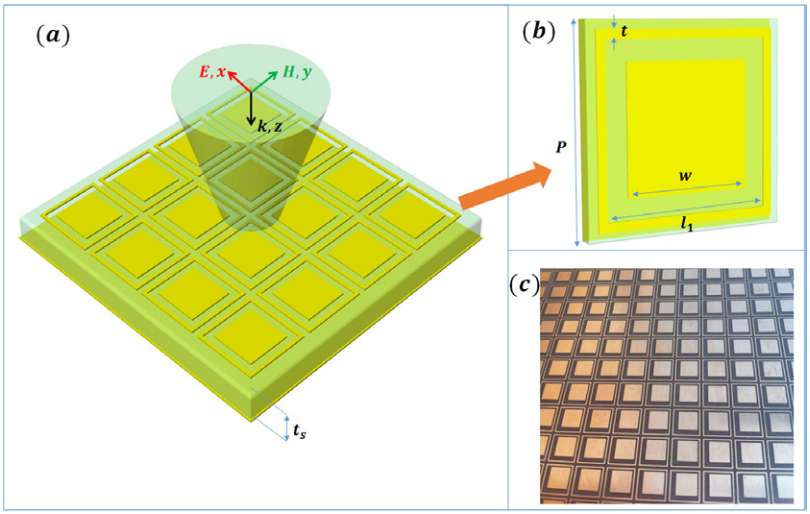

Figure 1. (a) Schematic of the MM absorber and polarization configuration of the incident EM wave, (b) Single unit cell of the designed MM absorber and (c) real sample.

Our simple MM-absorber design is composed of a copper-patterned layer at the front and continuous copper plane at the back, separated by a dielectric layer of FR-4. As shown in figures 1(a) and (b) the optimized unit cell is chosen as periodic dimensions of $p = 10\,\text{mm}$ in the x–y plane, and the thickness of dielectric layer is $t_s = 0.8\,\text{mm}$ in the propagation of EM wave, z direction. The front layer consists of an inner square with the length of $w = 6.2\,\text{mm}$, surrounded by an outer square ring with width and inner length of $t = 0.45\,\text{mm}$ and $l_1 = 8.2\,\text{mm}$, respectively.

The aforementioned geometrical parameters have been optimized by the commercial software CST Microwave Studio [18]. In the simulation, the conductivity of copper was $\sigma = 5.8 \times 10^7\,\text{S m}^{-1}$, and the FR-4 was simulated with a dielectric function of $\varepsilon = 4.3 \times (1 + 0.025i)$. The frequency domain solver was carried out with the periodic boundary conditions in the x–y plane and open for the z-direction to extract the S parameters. Owing to the polarized incident EM wave, the electric and the magnetic fields were parallel to x and y axes, respectively. Since transmission is eliminated by the continuous copper plane, which is much thicker than the penetration depth of copper at GHz frequency, then the absorption can be calculated by $A(\omega) = 1 - R(\omega) = 1 - |S_{11}(\omega)|^2$, where $A(\omega), R(\omega)$ are absorption and reflection coefficients, respectively. For the experimental process, the reflection spectra ($|S_{11}(\omega)|^2$) were measured in an anechoic chamber using Agilent E8364B network analyzer, which connected to linearly-polarized microwave standard-gain horn antennas [19]. At first, two antennas were placed at a proper distance (2.0 m from the sample to the middle point of two horn antennas) to neglect the overlapping effect between incident and reflected waves with the incident angle of 5°. The calibration was performed by replacing the sample (figure 1(c)) with a same size copper board as a perfect conductor. In the experiment of changing the incident angle, the distance between the two horn antennas and the distance between sample and two horn antennas were changed but still avoiding the overlapping effect.

The simulated and the measured absorption of the dual-band MM absorber is illustrated in figure 2(a). As aforementioned, two simulated peaks are obtained at 4.6 and 10.6 GHz with absorption of 99.5% and 77.2%, respectively. To be more detailed, the surface currents are illustrated in figure 2(b). One can clearly see that the peak at the lower frequency is mainly contributed by the outer square ring, and the inner square is mainly responsible for the peak at higher frequency. The second peak located at 10.6 GHz is easier to elucidate, which results simply from the magnetic response of the inner square: not only the strong anti-parallel surface currents between the inner square and continuous copper plane, but also rather weak anti-parallel currents between inner square and outer square ring. For the first absorption peak at 4.6 GHz with high absorption, the induced currents are mostly concentrated on the outer square ring. The strong induced currents at two sides of the outer square ring move in the opposite way to those in the corresponding continuous plane. Therefore, the first peak is a result of the magnetic resonance. At the same time, it should be mentioned that the strong parallel induced currents between two neighboring unit cells, which leads to a strong electric response. Then, the first peak is fully understood to be due to the magnetic and the electric resonances at the same frequency.

As reported, breaking the symmetry of a particular structure in MM allows us to access different resonant modes, which cannot be excited with symmetric configuration [20–22]. In our paper, even with the disadvantage of the low absorption for the second peak, we intend to change the coupling between two resonators (inner square and outer square ring) by changing the relative distances between them to seek the effect of symmetry breaking, leading us to higher absorption and more resonant modes.

The inner square shifts from the corner by displacement d in EM polarization as in figures 3(a) and (b). The evolution of absorption spectrum according to d is depicted in figures 3(c) and (d). The first absorption peak, as indicated to be due to the magnetic resonance and the electric response of outer

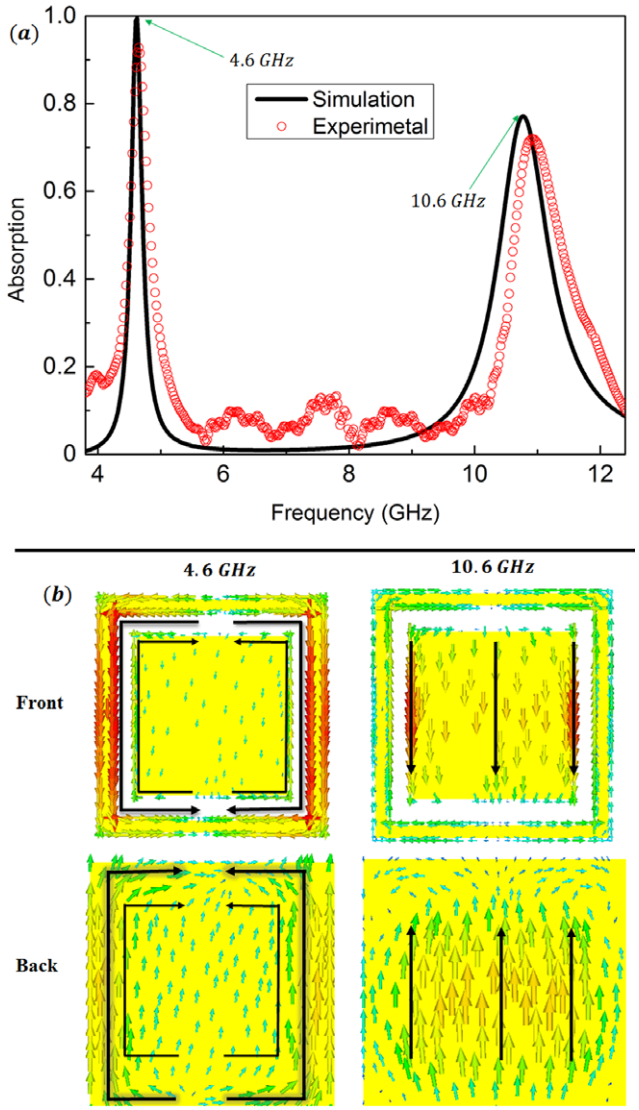

Figure 2. (a) Simulated and experimental frequency-dependent absorption for the symmetric MM absorber. (b) Induced surface currents at the two resonance frequencies. Black arrows show directions in the surface-current distribution.

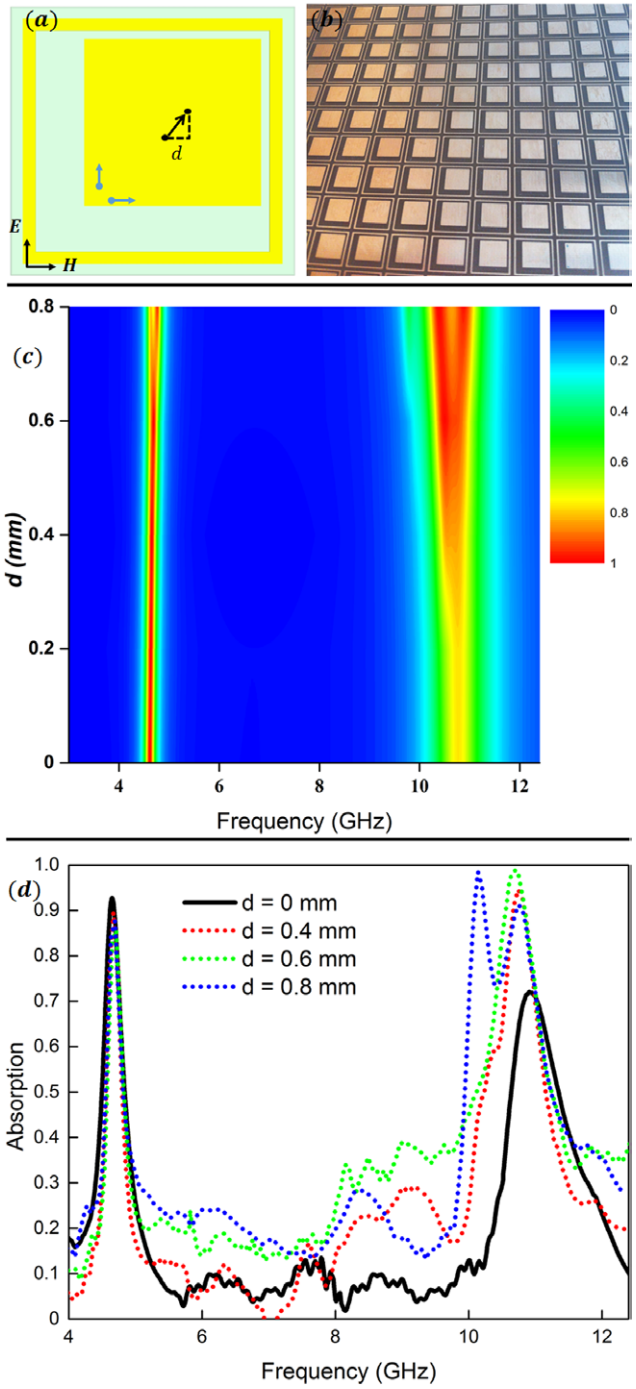

Figure 3. (a) Design of the unit cell for asymmetric MM absorber. (b) Photo of the fabricated sample. (c) and (d) Simulated and experimental frequency-dependent absorption for the asymmetric MM absorber.

square ring, shows a stable property even when d is increased. In other words, the first peak is nearly insensitive to the displacement of inner square. On the contrary, the second peak is significantly enhanced when d is increased. It is clearly seen that, for $d = 0.4$ mm, both absorption peaks are grown up to be higher than 90%, and the absorption peak at higher frequency with a full width at half maximum (FWHM) of 10%, in comparison with the symmetric structure (FWHM of 5%), shows broader absorption. When displacement d reaches 0.6 mm, the second peak starts to be separated into two peaks. As d is further increased, two peaks are clearly separated and, at $d = 0.8$ mm, our structure shows a triple-band absorption (TBA) at 4.6, 10.2 and 10.8 GHz with absorption higher than 94% for all the peaks.

We now clarify the resonances in order to further interpret the mechanism of our TBA structure. Figure 4 presents the behavior of EM wave to explain how it is absorbed in the MM slab at each resonance. At the beginning (the symmetric structure of $d = 0$), figure 4(a) shows the induced electric field, reaffirmed that the low and high absorption peaks are relevant, respectively, to the outer square ring and the inner square. In case of asymmetric structure ($d = 0.8$ mm), the first peak is nearly unchanged, but the induced electric field moves more or less along the ring within the thickness ($t = 0.45$ mm) of the outer square ring. At the same time, original single band at higher frequency is replaced by dual bands. The induced electric field of symmetric structure is positioned only in the

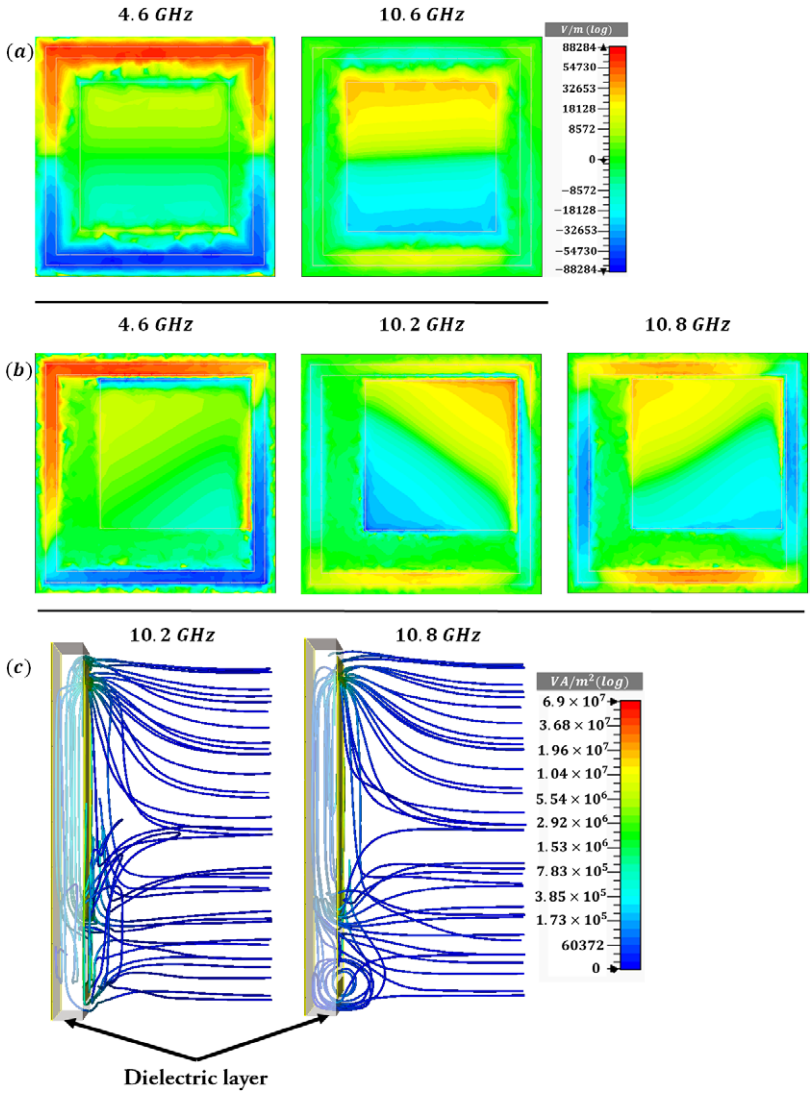

Figure 4. EM properties at each resonance: distributions of inducted field E_z of (a) symmetric structure (corresponding to the solid-black line in figure 3(d)) and (b) asymmetric structure with $d = 0.8$ mm (corresponding to the dotted-blue line in figure 3(d)). (c) Side view of the streamlines of the Poynting vector at two new resonances.

vertical direction (10.6 GHz in figure 4(a)), which leads to a single absorption peak. As shown in figure 4(b), for d of 0.8 mm, the induced electric field is degenerated into two diagonal modes on the inner square, resulting in two absorption peaks at 10.2 and 10.8 GHz. To elucidate the mechanism of two new absorption peaks, we show the completely 3-dimensional Poynting trajectory in figure 4(c). It is clear that the energy comes out from the transmitter port into the structure and is dissipated inside the dielectric layer. To summarize this paragraph, by simply changing the distance between inner square and outer square ring, dual/triple absorption bands could be controlled.

To understand the phenomenon of how symmetry breaking leads to splitting of the absorption peaks, we would like to explain under the analogous three-level system in quantum electromagnetically induced transparency (EIT) [23, 24]. Under the similar circumstance, the three-level system, which is depicted in figure 5, includes a ground state $|0\rangle$ and two upper states $|1\rangle$ and $|2\rangle$. With respect to the normal incident wave, at 10.6 GHz, the inner square is coupled with an excitation wave, giving rise to the absorption peak, called the bright element. This corresponds to

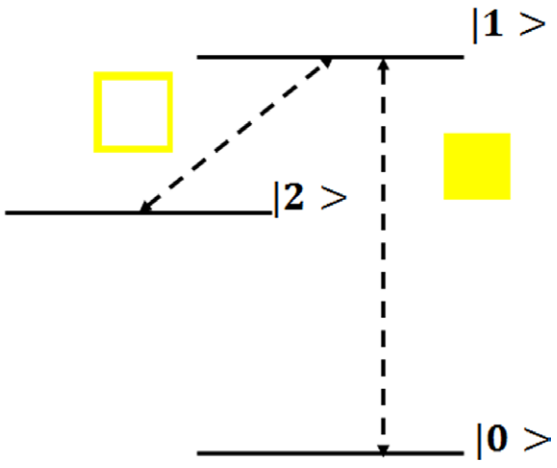

Figure 5. Three-level system of EIT.

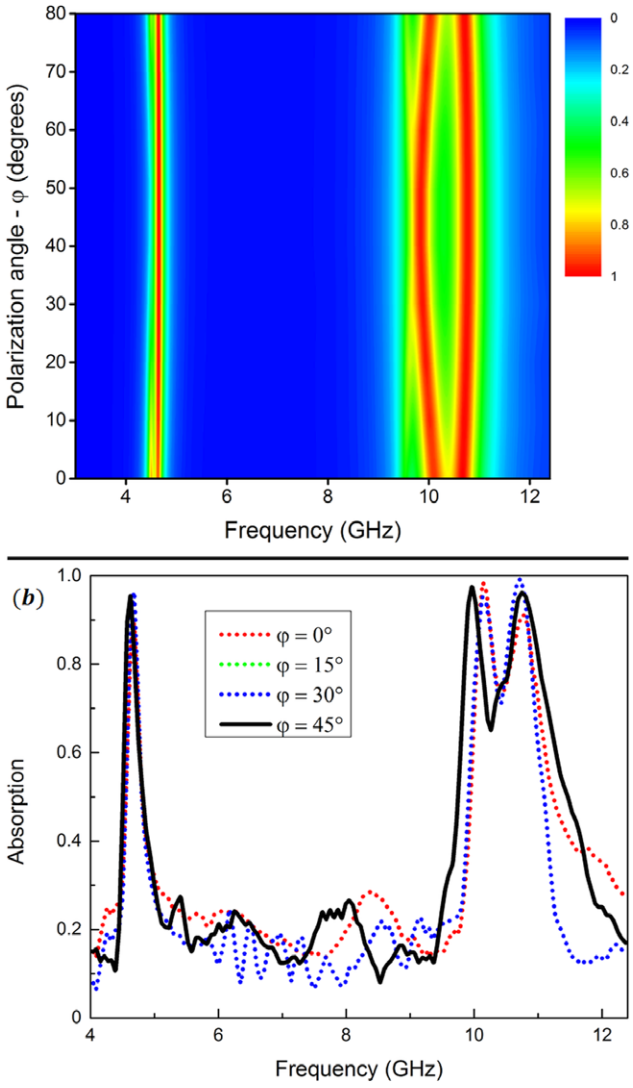

Figure 6. (a) Simulated and (b) experimental absorption spectra according to polarization angle.

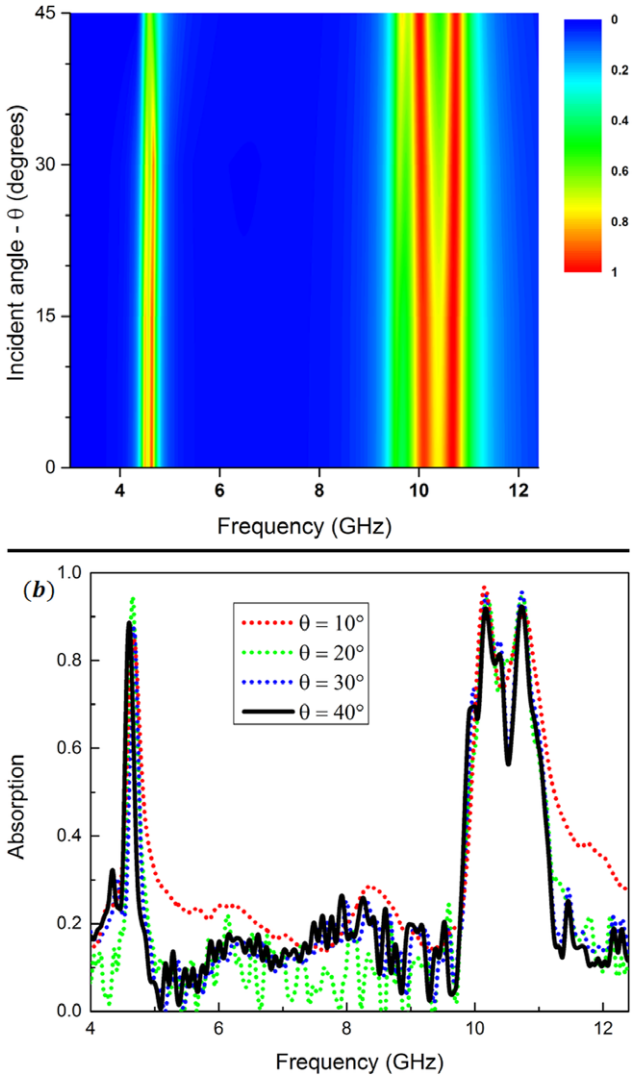

Figure 7. (a) Simulated and (b) experimental absorption spectra according to incident angle.

the dipole-allowed transition from $|0\rangle$ to $|1\rangle$. On the other hand, the outer square ring cannot be excited at 10.6 GHz and becomes the dark element or the dipole-forbidden transition of $|0\rangle$ to $|2\rangle$. Therefore, only single peak is observed at 10.6 GHz. Nevertheless it is suggested that, the dark element can be strongly coupled with the bright element by near-field coupling between them, which causes the splitting of the resonance peak. By breaking structural symmetry, that is, at $d = 0.8$ mm, the initial absorption peak splits into dual-band absorption at 10.2 GHz and 10.8 GHz. The observed dual-band absorption is the result of coupling between the dipole (the inner square) and the quadrupole (the outer square ring). The absorption mechanism is clarified by the electric-field distribution in figure 4. When $d = 0$, the electric response of the outer square ring is weak at 10.6 GHz, no coupling effect is observed. When $d = 0.8$ mm, as shown in figure 4(b), a electric quadrupole is formed and strongly coupled with the dipole in the inner square by the near-field coupling. Consequently, the EM field is trapped at 10.2 and 10.8 GHz. The harmonic oscillator model is widely used in EIT to quantitatively analyze the coupling effect. The interaction between two oscillators can be described by the following equations [24].

$$\ddot{x}_1(t) + \gamma_1\dot{x}_1(t) + \omega_0^2 x_1(t) + \tau^2 x_2(t) = q_1 E_0, \tag{1}$$

$$\ddot{x}_2(t) + \gamma_2\dot{x}_2(t) + \omega_0^2 x_2(t) + \tau^2 x_1(t) = q_2 E_0 = 0, \tag{2}$$

where x_1 and x_2 are the amplitudes of oscillator 1 (bright mode) and oscillator 2 (dark mode), γ_1 and γ_2 are the losses of oscillators 1 and 2, respectively. τ is the coupling coefficient describing the coupling strength between two oscillators, ω_0 is the resonance frequency of oscillator 1, and q_1, q_2 are the coupling strength of bright and dark modes with incident wave, respectively. Here, $q_2 = 0$. According to equations (1) and (2), two stop bands are obtained [24]:

$$\omega_- = \sqrt{\omega_0^2 - \tau^2} \tag{3}$$

and

$$\omega_+ = \sqrt{\omega_0^2 + \tau^2}, \tag{4}$$

where ω_- and ω_+ are the mode of two new absorption peaks, the width of the new band is:

$$\Delta\omega = \omega_+ - \omega_- \approx \frac{\tau^2}{\omega_0}. \quad (5)$$

It is simple to see that when the coupling coefficient is increased or when d is increased, two absorption peaks are more separated, which makes the spectrum broader. A similar observation is found in figure 3(d).

To investigate the polarization insensitivity of the suggested MM structure, we measured the absorption spectra according to polarization angle. Figures 6(a) and (b) present the simulated and the experimental absorption spectra as the polarization angle increases from 0 to 80° and from 0 to 45°, respectively. Polarization angle φ is the angle between x-axis and electric field of the incident EM wave. Our structure is composed of two elements, which are inner square and outer square ring with high-degree symmetry (4-fold symmetric structure), then changing the polarization of incident EM wave is expected to be insensitive to the absorption. As shown in figure 6(a), the absorption peak is nearly unchanged when polarization is increased. In addition, the polarization independence is also revealed in the experiment.

For the discussion so far, the normal incidence has been applied to achieve the MM absorber. In real applications, EM wave is usually incident onto the absorber at an oblique angle. Therefore to study this case, we focus on asymmetric structure with $d = 0.8$ mm under oblique incidence. Figures 7(a) and (b) show the simulated and the experimental absorption spectra as the incident angle increases from 0 to 45° and 0 to 40°, respectively. The absorption is maintained to be higher than 90% for incident angle up to 40°. As reported in [25], the magnetic resonance is nearly unchanged when H is fixed. These results indicate that our suggested MM structure reveals wide incident-angle independence, which is valuable for real applications.

In conclusion, dual/triple-band MM absorber was numerically and experimentally demonstrated by controlling the symmetry of a simple structure. The shift of inner square makes the second resonance mode split into two absorption peaks, and furthermore the absorption of TBA is higher than 94%. The TBA is also clarified to be insensitive to the polarization of incident wave and can work even for incident angle up to 40°. Our work promises for advanced applications, especially, filtering and detecting devices.

Acknowledgments

This work was supported by the ICT R&D Program of the MSIP/IITP, Korea (KCA-2013-005-038-001).

References

[1] Basiri R, Abiri H and Yahaghi A 2014 *Microw. Opt. Technol. Lett.* **56** 636
[2] Liu N, Weiss T, Mesch M, Langguth L, Eigenthaler U, Hirscher M, Sönnichsen C and Giessen H 2009 *Nano Lett.* **10** 1103
[3] Schittny R, Kadic M, Bückmann T and Wegener M 2014 *Science* **345** 427
[4] Melik R, Unal E, Perkgoz N K, Puttlitz C and Demir H V 2009 *Appl. Phys. Lett.* **95** 181105
[5] Tung N T, Tung B S, Janssens E, Lievens P and Lam V D 2014 *J. Appl. Phys.* **116** 083104
[6] Lam V D, Kim J B, Tung N T, Lee S J, Lee Y P and Rhee J Y 2008 *Opt. Express* **16** 5934
[7] Jin X-R, Park J W, Zheng H, Lee S J, Lee Y P, Rhee J Y, Kim K W, Cheong H S and Jang W H 2011 *Opt. Express* **19** 21652
[8] Shalaev V M 2007 *Nat. Photonics* **1** 41
[9] Rhee J Y, Yoo Y J, Kim K W, Kim Y J and Lee Y P 2014 *J. Electromagn. Waves Appl.* **28** 1541
[10] Landy N I, Sajuyigbe S, Mock J J, Smith D R and Padilla W J 2008 *Phys. Rev. Lett.* **100** 207402
[11] Wang B-X, Wang L-L, Wang G-Z, Huang W-Q, Zhai X and Li X-F 2014 *Opt. Commun.* **325** 78
[12] Cao T, Wei C-W, Simpson R E, Zhang L and Cryan M J 2014 *Sci. Rep.* **4** 3955
[13] Tuong P V, Park J W, Rhee J Y, Kim K W, Jang W H, Cheong H and Lee Y P 2013 *Appl. Phys. Lett.* **102** 081122
[14] Yoo Y J, Zheng H Y, Kim Y J, Rhee J Y, Kang J-H, Kim K W, Cheong H, Kim Y H and Lee Y P 2014 *Appl. Phys. Lett.* **105** 041902
[15] Yoo Y J, Kim Y J, Van Tuong P, Rhee J Y, Kim K W, Jang W H, Kim Y H, Cheong H and Lee Y P 2013 *Opt. Express* **21** 32484
[16] Ayop O B, Rahim M K A, Murad N A, Samsuri N A and Dewan R 2014 *Prog. Electromagn. Res. M* **39** 65
[17] Park J W, Tuong P V, Rhee J Y, Kim K W, Jang W H, Choi E H, Chen L Y and Lee Y P 2013 *Opt. Express* **21** 9691
[18] Computer Simulation Technology 2015 (Framingham, CA: CST) http://cst.com
[19] Engheta N and Ziolkowski R W 2006 *Metamaterials: Physics and Engineering Explorations* (New York: Wiley)
[20] Aydin K, Pryce I M and Atwater H A 2010 *Opt. Express* **18** 13407
[21] Christ A, Martin O J, Ekinci Y, Gippius N A and Tikhodeev S G 2008 *Nano Lett.* **8** 2171
[22] Fedotov V, Rose M, Prosvirnin S, Papasimakis N and Zheludev N 2007 *Phys. Rev. Lett.* **99** 147401
[23] Zhu L and Dong L 2014 *J. Opt.* **16** 125105
[24] Meng F Y, Wu Q, Erni D, Wu K and Lee J C 2012 *IEEE Trans. Microw. Theory Tech.* **60** 3013
[25] Dung N V, Yoo Y J, Lee Y P, Tung N T, Tung B S and Lam V D 2014 *J. Korean Phys. Soc.* **65** 70